Investigate the effect of co-doping on the grain size and diffuse phase transition of barium titanate ceramics

M. S. Alkathy[a], J. P. Goud[b], K. E. Ibrahim[c], H. A. Kassim[d,*]
[a]*Department of Physics / CCET / Federal University of São Carlos, CEP 13565-905, São Carlos-SP, Brazil*
[b]*Department of Physics, Koneru Lakshmaiah Education Foundation, Bowrampet, Hyderabad, 500043, Telangana, India*
[c]*Department of Zoology, College of Science, King Saud University, P.O. Box 2455, Riyadh 11451, Saudi Arabia*
[d]*Department of Physics, College of Science, P.O. BOX 2455, King Saud University, Riyadh 11451, Saudi Arabia*

An investigation examined the impact of co-doping $BaTiO_3$ ceramics with La^{3+} and Nd^{3+} on their microstructural, dielectric, and phase transition properties. The synthesis of $BaTiO_3$ with co-doping of La^{3+} and Nd^{3+}, using the general formula $Ba_{1-x}(La_{1/3}, Nd_{1/3})_xTiO_3$ (BLNdTx) with varying concentrations of x (0%, 2%, 4%, and 8%), is achieved by the solid-state reaction technique. A temperature-dependent dielectric permittivity investigation was conducted at four distinct frequencies (1 kHz, 10 kHz, 100 kHz, 500 kHz, and 1 MHz) within the 30–200 °C temperature range. The findings indicate that the samples show a diffuse phase transition and a noticeable divergence from the typical Curie-Weiss equation. The diffuseness parameters γ for phase transition rose from 1.15 to 1.75 as x grew from 0 to 8%, respectively. The concurrent impact of surface phenomena, mechanical stress phenomena, and the external effect of grain boundaries might explain the substantial size reduction. An in-depth understanding of the grain size effect and its underlying mechanism would be advantageous for advancing and practically using $BaTiO_3$-based ceramics and other ferroelectrics.

(Received April 21, 2024; Accepted July 22, 2024)

Keywords: Barium titanate, Co-doping, Grain size effect, Diffuse phase transition

1. Introduction

Ferroelectric materials have a natural dielectric polarization, known as Ps, which may be reversed by applying an electric field [1-3]. The movement of the charge centers about each other or the arrangement of charges results in the creation of electric dipoles. Barium titanate is the first ferroelectric perovskite ceramic that was found. It has a high dielectric constant and undergoes three structural phase changes [4]. The ferroelectric phase transitions of $BaTiO_3$ (BT) are linked to its consecutive aberrations in the crystal structure [5-7]. BT's high dielectric constant and modest dissipation factor make it well-suited for multilayer capacitor applications [8]. Several parameters, including synthesis process, purity, grain size, density, sintering temperature, frequency, doping, and substitution, may affect the dielectric characteristics of BT [9]. Recently, ferroelectrics with diffused phase transition have gained significant interest in basic research and industrial applications [10-12]. This is due to their ability to operate across a more comprehensive temperature range than typical ferroelectrics in capacitor applications. Several ferroelectric compositions display a broad dielectric peak at the temperature Tm, independent of frequency [13-18]. The materials in question are classified as ferroelectrics exhibiting a diffused phase transition, often called FE-DPT [19]. The extent of spreading in the phase transition peak is a significant property of these transitions. The cause of diffused ferroelectric phase transition often needs to be clarified [20-22]. However, it is believed to be linked to defects in the materials caused by

* Corresponding author: hkassim@ksu.edu.sa
https://doi.org/10.15251/JOR.2024.204.513

variations in composition, chaos in the arrangement of positively charged ions, the structure of the grains, minor imperfections, and microscopic differences [23]. The relaxor polarization of defects in FE-DPT affects the total dielectric permittivity and the overall form of the dielectric response [24-26]. Lithium sodium niobate (LNN) ceramics are significant in resonator and filter applications. They display a phenomenon called DPT, caused by the disorder in composition resulting from several kinds of cations occupying an equivalent site in the lattice [27]. Most substituted BT compositions exhibit a dispersed phase transition that deviates from the Curie-Weiss equation throughout a wide range of temperatures and frequency dispersion [28-30]. Based on the literature mentioned above and in the same direction, this paper investigates the effect of La^{3+} and Nd^{3+} co-doped on the diffused phase transition of $BaTiO_3$ ceramics. The ceramics were synthesized utilizing a solid-state reaction. The study focuses on the impact of these compositions on temperature-dependent dielectric permittivity. The findings indicate that including La^{3+} and Nd^{3+} in $BaTiO_3$ demonstrates an intriguing characteristic: the displacement of the phase transition towards a higher temperature range. This adjustment is seen as beneficial for enhancing the stability of the dielectric's capacitance at high temperatures. The research introduces a novel exploration into the effects of co-doping $BaTiO_3$ ceramics with La^{3+} and Nd^{3+}. While previous studies have examined individual dopants, the combined influence of La^{3+} and Nd^{3+} on the diffused phase transition of $BaTiO_3$ is relatively unexplored. The study suggests that incorporating La^{3+} and Nd^{3+} leads to a displacement of the phase transition towards lower temperatures, potentially enhancing the stability of the dielectric's capacitance at elevated temperatures. This advancement could have significant implications for applications requiring reliable operation under harsh conditions. Additionally, understanding the influence of these dopants on dielectric properties across various temperature ranges is crucial for customizing materials for specific uses.

2. Experimental

The $BaTiO_3$ samples were synthesized using a conventional solid-state technique, with co-substitution of La^{3+} and Nd^{3+}. The samples were prepared using the general formula $Ba_{1-x}(La_{1/3},Nd_{1/3})_xTiO_3$, referred to as (BLNTx), with x values of 0, 2%, 4%, and 8%. The $BaTiO_3$ powder, co-doped with La^{3+} and Nd^{3+} ions, was synthesized using high-purity $BaCO_3$, La_2O_3, Nd_2O_3, and TiO_2 as starting components. The $BaCO_3$ and TiO_2 had purities of 99.99%, while the La_2O_3 and Nd_2O_3 had purities of 99.98%. The combination was pulverized and, after that, subjected to ball milling for 12 hours. Afterward, the powdered material was calcinated in a standard furnace at 1100°C for 8 hours, using a heating and cooling rate of 5°C per minute. The powder was compressed using a 1% concentration of polyvinyl alcohol (PVA) as a binder at a unidirectional pressure of 90 MPa, resulting in pellets measuring 1 mm in height and 8 mm in diameter. The pellets were heated at a temperature of 500°C for 1 hour to eliminate the binder. This was accomplished using a muffle furnace with a heating and cooling rate of 2°C per minute. Ultimately, the samples were subjected to sintering in the presence of air at a temperature of 1350°C for 5 hours. This process was carried out using a typical furnace with a heating and cooling rate of 5°C per minute. The morphological structure was examined using scanning electron microscopy. To evaluate the dielectric properties, a coating of silver paste was evenly spread on both surfaces of the sample discs, forming a capacitor-like structure. The dielectric permittivity properties of the sintered samples were assessed using an impedance analyzer, especially the Agilent E4292A, throughout a temperature range of 30-200°C at different frequencies.

3. Results and discussion

Figure 1 displays the scanning electron microscope (SEM) images of BLNTx sintered ceramics, where x represents 0, 2%, 4%, and 8%. It has been noted that all sintered samples had a very dense microstructure. However, the microstructure of the co-doped samples was even more compact, with a smaller grain size than the pure sample. The densities of all samples were

determined using the Archimedes technique [31], and the values obtained confirm the microstructure seen by FE-SEM. The sintered samples have relative densities of over 95%. Furthermore, based on the same data, it is evident that the density of ceramics experiences a tiny drop when the concentration of La^{3+} and Nd^{3+} rises. The pure sample exhibited a slightly higher density value than the co-substituted samples. This finding aligns with the literature that documents the investigations of La-doped $BaTiO_3$ ceramics [32-33]. The La^{3+} and Nd^{3+} ions function as donors and take the place of Ba^{2+} ions in the lattice structure. This substitution may cause lattice distortion owing to the development of vacancies and the difference in size between the La^{3+}, $Nd^{3+,}$ and Ba^{2+} ions. The latter may impede mass transportation in dense buildings and hinder densification [32-33]. The line intercept with the assisting ImageJ technique [34], confirmed from grain size distribution in the inset photos in Figure 1, was used to determine the average grain sizes of the ceramics. The results showed that the average grain sizes were around 5.5 µm, 2.5 µm, 1.85 µm, and 1.1 µm for La^{3+} and Nd^{3+} co-doping concentrations of x = 0, 2%, 4%, and 8%, respectively. As the levels of La^{3+} and Nd^{3+} in $BaTiO_3$ ceramics rose, it was observed that the formation of grains was inhibited. The decrease in grain size resulting from including La^{3+} and Nd^{3+} ions may be ascribed to the impurity drag mechanism in solid solution, where a gradient of La^{3+} and Nd^{3+} ions is present at the borders between grains. The reduction in grain size may be attributed to the presence of La^{3+} and Nd^{3+} ions, which likely hindered the development of the grains by impeding the movement of the grain border. This finding is consistent with the information presented in the literature on La^{3+}-doped $BaTiO_3$ [32-33].

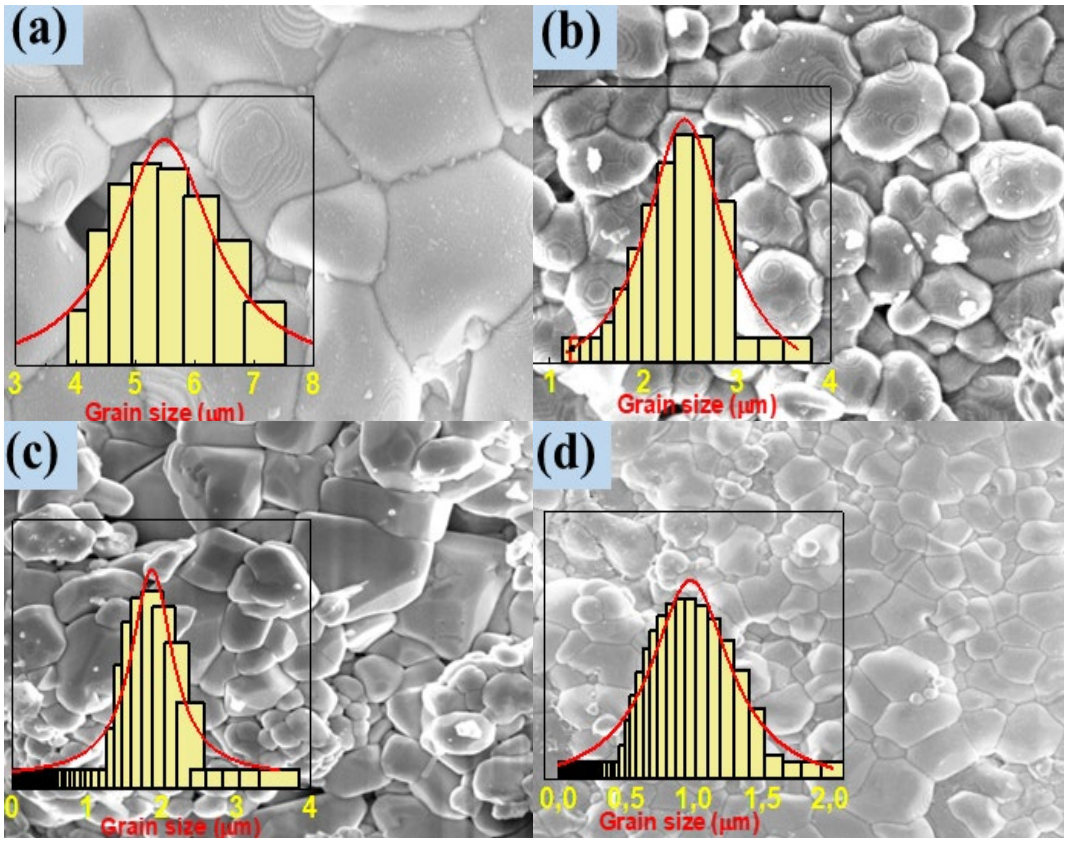

Fig. 1. SEM image and schematic diagram of the grain size distribution of BLNTx ceramics measured with a High-resolution scanning electron microscopy.

An EDS mapping investigation was performed on 8% La3+ and Nd3+ co-doped $BaTiO_3$ ceramic material to determine its constituent makeup. Figure 2 displays the results of the measurements. The chosen area showed no segregation in the distribution of five primary elements

(Ba, Ti, La, Nd, and O). This result demonstrates that the 8% co-doping concentration of Nd^{3+} and Li^{+} ions was sufficient to completely dissolve and integrate the doped ions into the $BaTiO_3$ lattice. By focusing on the 8% composition, we may efficiently devote resources to conduct detailed research of the material's elemental properties at a critical doping level. The optimized physical properties at this doping level were a significant factor in concentrating on the 8% La^{3+} and Nd^{3+} dopant composition. As highlighted in our study, this composition demonstrated superior performance regarding small grain size, diffused phase transition, high breakdown strength, high energy storage density, and efficiency. Additionally, we acknowledge the importance of verifying the formation of a single phase, especially at higher dopant concentrations. To address this, we incorporate additional microstructure mapping at elevated dopant contents in this work. This inclusion aims to provide a more comprehensive understanding of the material's structural integrity and phase purity across a broader, higher-dopant range. This modification will contribute to a more robust interpretation of the material's elemental composition and structural characteristics.

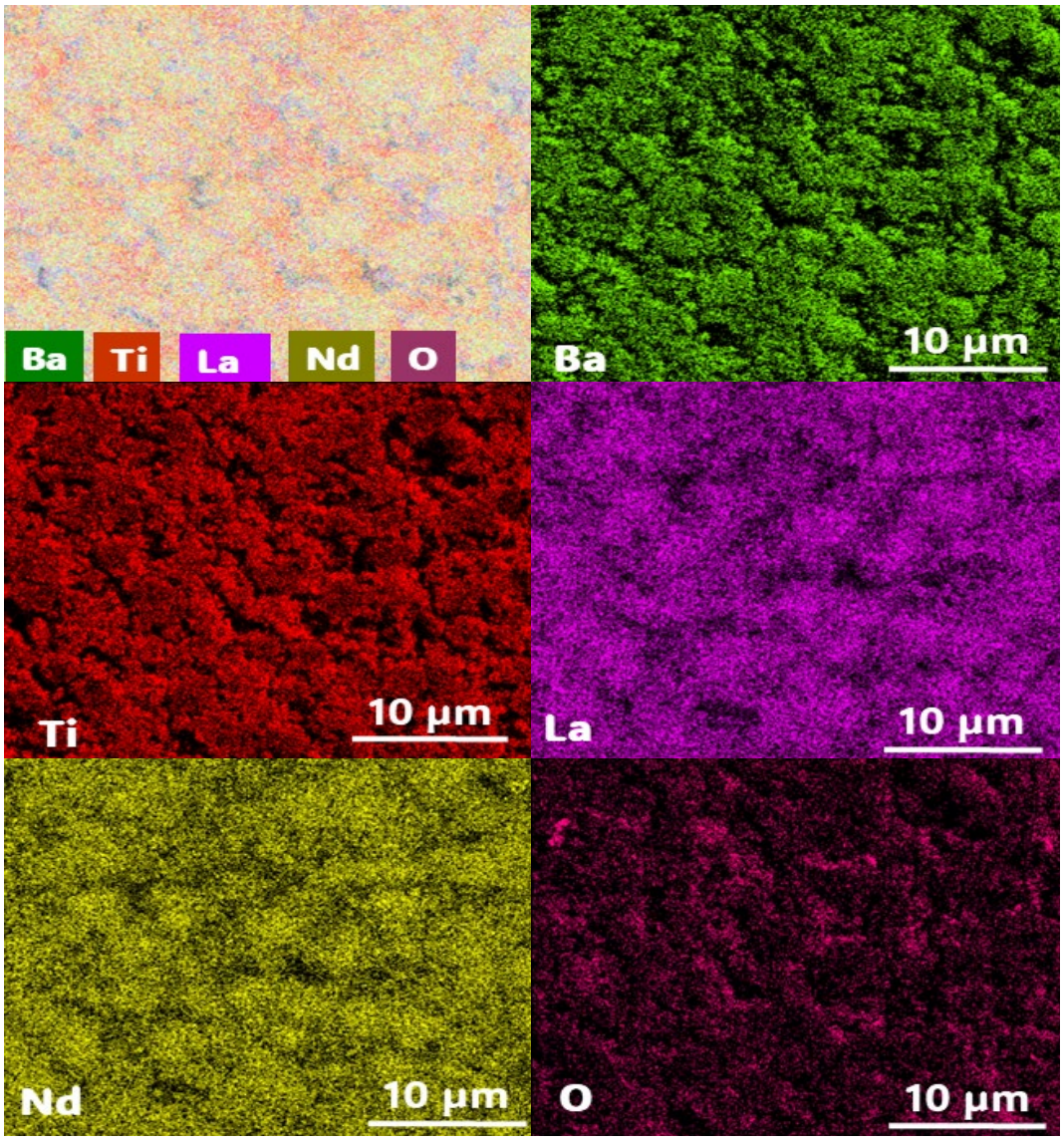

Fig. 2. EDS elemental mapping images of BLNT8% ceramic sample.

The temperature dependence of the dielectric constant and dielectric loss of BLNTx ceramics was studied at different frequencies, namely 1 kHz, 10 kHz, 100 kHz, 500 kHz, and 1 MHz, and in the temperature range of 25–200 °C, as shown in Figure 3(a)-3d). It can be observed from Figure 2(a) that the dielectric constant for x = 0, x =2%, and x =4% gradually increased and reached a maximum value at a specific temperature defined as Curie temperature and then decreased. This indicates the phase transition from ferroelectric to paraelectric state [35-36]. However, for the sample of La^{3+} and Nd^{3+} co-doped $BaTiO_3$ ceramics with x =8%, the maximum value of the dielectric constant remained high value over a higher range of temperature and increased slightly at Tc~90 ºC, which confirms that the sample has such diffused phase transition behavior. Differences in grain size and a gradient of quadraticity are responsible for the diffuse character of ferroelectric ceramic transitions, leading to a broad spectrum of transition temperatures. The large range of phases seen in ceramics is due to various variables. Due to changes in microscopic composition, micropolar regions are merging into micropolar areas, and due to local strain, the order parameter is connected to the local disorder mode [37].

Vugmeister [38] demonstrated that the fundamental reason for DPT behavior in mixed oxide compounds is the random distribution of the electrical strain field. When aliovalent cations are introduced into a perovskite structure, they may change the electrical characteristics by acting as electron donors or acceptors, respectively. This finding persists, although these ions are insoluble due to their positive charges [39]. According to Watanabe et al. [40], three primary steps exist in replacing rare earth elements in $BaTiO_3$. Doping involves substituting ions for those that had previously occupied the A or B positions of the lattice. It has been shown that the A and B sites in BT solid solutions are consistent with the ionic radii of La^{3+} and Nd^{3+}. Watanabe et al. [40] observed that the first phase of the reaction might be described by substituting La^{3+} and Nd^{3+} ions for Ba^{2+} ions. Shannon states that La^{3+} and Nd^{3+} ions benefit from having a lower ionic radius [41]. Therefore, introducing La^{3+} and Nd^{3+} ions with different contents, x = 0.02, x = 0.04, and x = 0.08, leads to a change in the lattice structure. Internal stresses increase because of lattice constriction, smaller grains, and smaller grain boundary areas, as seen in scanning electron microscopy (SEM) images. This process can potentially cause chemical heterogeneity on the nanoscale, leading to a dispersion of several local Curie values [42-47]. The constant increase in dielectricity with temperature could be due to the orientation polarization of the dipoles' thermal motion. At lower temperatures, it isn't easy to orient the dipoles spontaneously, but it becomes more accessible when the temperature rises. Thus, the orientation polarization will increase, increasing the dielectric constant value [48-49]. The decrease of dielectric constant after Curie temperature is due to the phase transition of the crystal structure from a tetragonal phase to a cubic phase [50-51].

Furthermore, the decrease in dielectric constant could be because of the increasing thermal oscillations of the molecules, which can lead to an increase in the degree of dipole disordering in the cubic phase [52]. Also, we can see in Figure 3(a)-(d) that the Curie temperature shifted toward the lower temperature side with an increase in dopant concentrations. The shifting in the Curie temperature (Tc) of $BaTiO_3$ ceramics due to co-doping with La^{3+} and Nd^{3+} may be ascribed to many variables. The search results did not explicitly address the factors influencing the alteration of the Curie temperature in $BaTiO_3$ ceramics when rare-earth ions are introduced. However, existing research and expertise in the area indicate that the following variables might potentially impact this phenomenon: (i) Interactions amongst Dopant Ions: The inclusion of La^{3+} and Nd^{3+} ions might result in interactions with the BTO host lattice, which can impact the crystal structure and ferroelectric properties of the material, thereby impacting the Curie temperature [53]. La^{3+} doping may alter the crystal structure of $BaTiO_3$, influencing the Curie temperature of the material [54]. The dielectric characteristics of the material may be altered by the La^{3+} and Nd^{3+} ions, leading to a change in the Curie temperature [55]. Doping Concentration: The magnitude of the change in the Curie temperature may also be influenced by the concentration of La^{3+} and Nd^{3+} doping, where larger doping concentrations result in a more pronounced reduction in the Curie temperature [56, 57]. The search results provided a general understanding of the behavior of Curie temperature in doped ceramics. However, they lacked specific information on the precise parameters that induce the shift when La^{3+} is introduced to $BaTiO_3$. Hence, the criteria are derived from the current comprehension of dopant ions' impact on ferroelectric materials' characteristics.

Researchers and scientists require further investigation to comprehensively understand the mechanism behind the change in Curie temperature when La^{3+} and Nd^{3+} are introduced into $BaTiO_3$ ceramics.

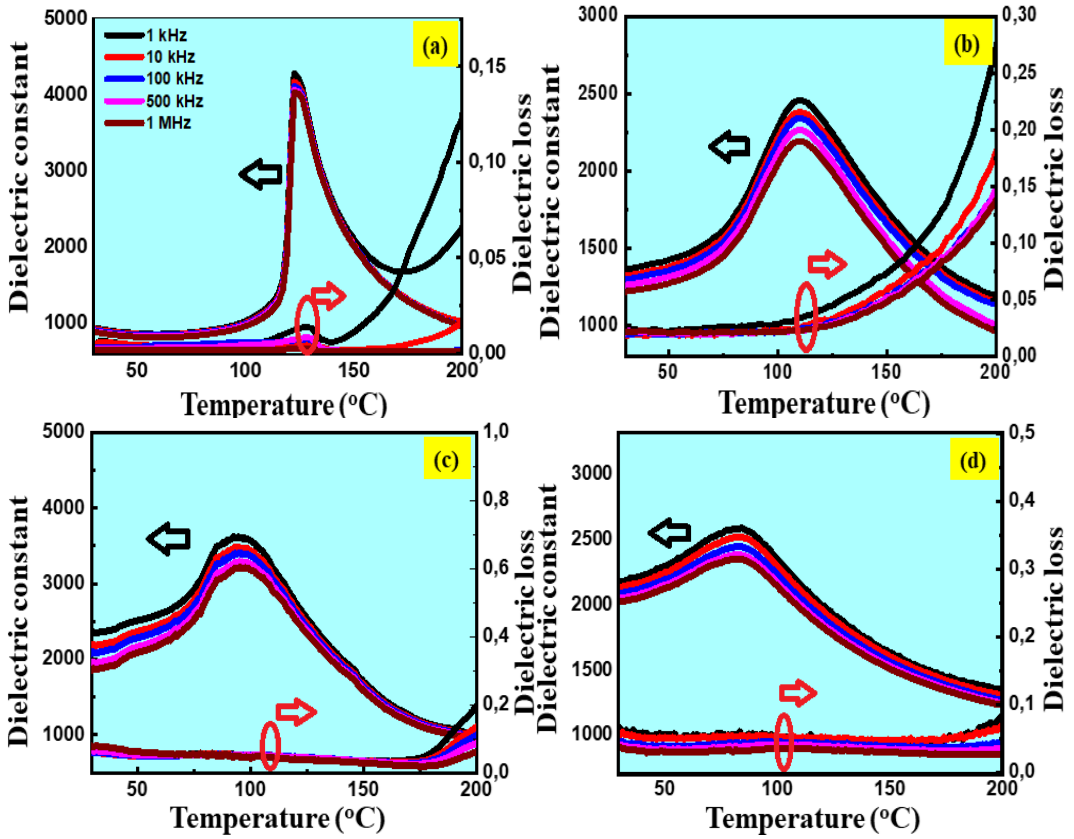

Fig. 3. Temperature-dependent dielectric constant and loss tangent of sintered BLNTx ceramics; (a) x=0, (b) x=0.02, (c) x=0.04, and (d) x=0.08. To determine its temperature dependency, the measurement was tested at five different frequencies, namely f=1 kHz, 10 kHz, 100 kHz, 500 kHz, and 1 MHz.

To thoroughly examine the dielectric dispersion and diffusiveness of the investigated samples, we have plotted the modified version of the Curie-Weiss equation [58].

$$\frac{1}{\varepsilon} - \frac{1}{\varepsilon_m} = \frac{(T-T_m)^\gamma}{c} \tag{1}$$

C stands for a constant in this instance. Simultaneously, γ is used to quantify the degree of diffuseness over the change from the ferroelectric to the paraelectric phase. At temperature T, the dielectric permittivity is represented by the symbol ε_r, while at temperature T_m, it is defined by the sign ε_m. In addition to the constant C, the equation also includes the degree of diffuseness γ, where γ may take on values ranging from 1 in normal ferroelectric to 2 in relaxor ferroelectric. Figure 4(a)-(d) shows the samples prepared at a frequency of 10 kHz versus the natural logarithm of the difference between the measured and actual temperatures, where the relative permittivity is subtracted from the measured permittivity. The slopes of the graphs may be used to determine the diffuseness degree (γ) values since the charts show a linear association and equation (1) is used. Based on a value of γ = 1.15, this investigation found that the pure $BaTiO_3$ sample (x = 0.0) had typical ferroelectric behavior. Nevertheless, the value of γ rose steadily from 1.10 to 1.75 when the $BaTiO_3$ co-doped with La^{3+} and Nd^{3+} grew to 8%. The diffuseness of phase transition becomes

more apparent when the co-doping concentration increases, and the difference in ionic radii between the host and dopant ions and cation disordering is responsible for the increased diffuseness [59, 60]. Co-doping La^{3+} and Nd^{3+} can improve the dielectric thermal stability behavior, which shows great promise for energy storage technology [61, 62]. La^{3+} as a single dopant [63, 64] increases the diffuseness of phase transitions, indicating the formation of diffuse ferroelectric material, but in co-doped ceramics, the diffuseness is even higher [63, 64]. Doping La^{3+} and Nd^{3+} ions in place of Ba^{2+} in the $BaTiO_3$ lattice improves the dielectric and ferroelectric properties and the maximized breakdown strength, attributed to enhanced energy storage performance.

The search results include data about the impact of grain size on the dielectric characteristics of doped barium titanate ($BaTiO_3$) materials, particularly with La^{3+} and Nd^{3+} doping. The research indicates that the size of the grains impacts the diffuse phase transition of $BaTiO_3$. Larger grain sizes are linked to a more noticeable ferroelectric transition, whereas smaller grain sizes display diffuse phase transitions. Naik et al. observed and documented the relationship between transition temperature and size effect in thin films. They proposed that inter-grain stresses may contribute to the greater transition temperature in thin films than in bulk ceramics [65]. The thin film works often display diffuse phase transition in polar clusters, whereas doped $BaTiO_3$ compositions do not show the presence of polar clusters [65, 66]. Liu et al. studied the structural development and dielectric characteristics of $BaTiO_3$ ceramics co-doped with Nd^{3+} and Mn. They discovered that when the Nd^{3+} concentration increased, the grain size and dielectric constant decreased [67]. Similarly, Gong et al. conducted a study on ceramics of $BaTi_{0.96}Mn_{0.04}O_3$ with La^{3+} substitution at the A-site. Their objective was to determine the ferromagnetic origin, and they discovered that the grain size reduced as the La^{3+} concentration increased [68]. The results indicate that the size of the grains impacts the diffuse phase transition of $BaTiO_3$. Larger grain sizes are linked to a more noticeable ferroelectric transition, whereas smaller grain sizes show diffuse phase transitions. The search results need to mention the methods via which the grain size influences the diffuse phase transition of La^{3+} and Nd^{3+} doped $BaTiO_3$. Additional investigation is required to comprehensively understand the correlation between the size of grains and the diffuse phase transition in doped barium titanate materials.

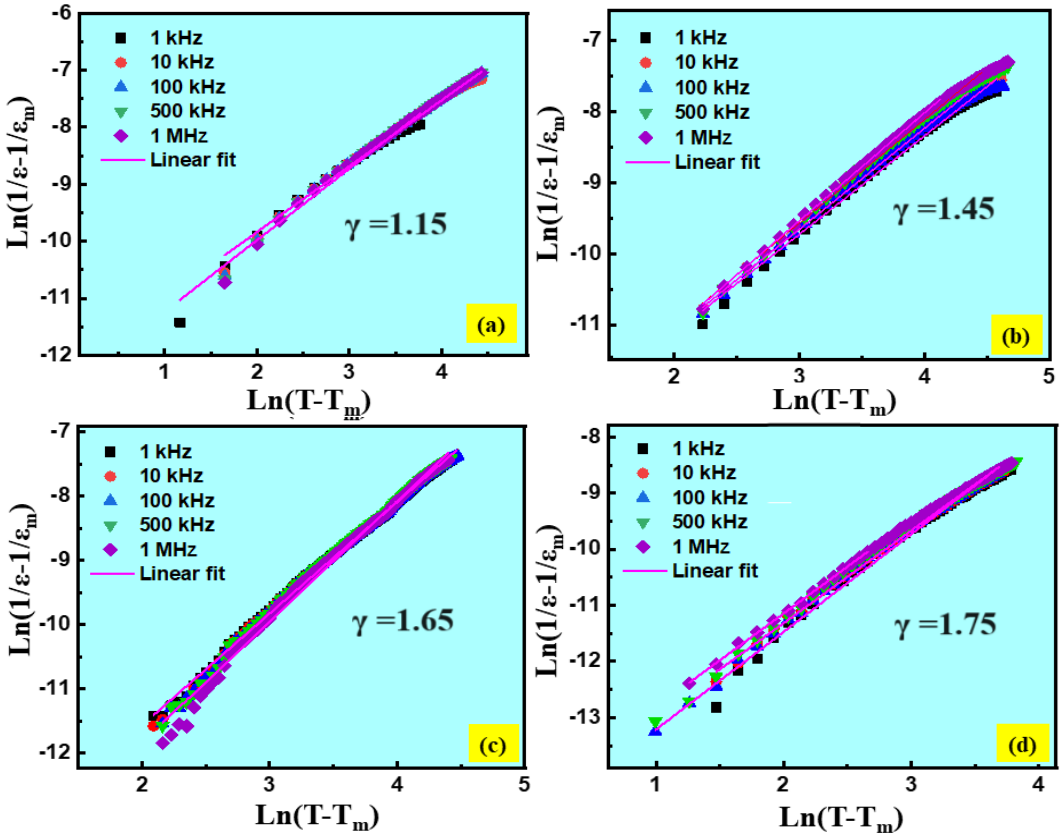

Fig. 4. Indicated to the empirical formal relationship of modified Curie Weiss law fitted to estimate the degree of diffuseness caused by La and Nd co-doped $BaTiO_3$ ceramics (a) x = 0.0, (b) x = 0.02, (c) x = 0.04, and (d) x = 0.08 measured at five different frequencies.

4. Conclusion

Overall, this study has provided insight into how adding La and Nd to $BaTiO_3$ ceramics affects their microstructure, dielectric characteristics, and phase transitions. Using the BLNdTx formula, we successfully synthesized $BaTiO_3$ with co-doped La and Nd. We varied the x amounts to show that it is possible to customize the material characteristics using the solid-state reaction approach. Our study on the dielectric properties of the samples, which included measuring the changes in electrical polarization with temperature and frequency, showed the occurrence of diffuse phase transitions. Additionally, we observed a significant deviation from the expected behavior described by the Curie-Weiss equation. In addition, our results indicate that the diffuseness parameters γ for phase transition rose as the concentrations of co-dopants increased, suggesting a more diffuse phase transition behavior. This behavior may be attributed to the combined impact of surface phenomena, mechanical stress phenomena, and the influence of grain boundaries. Comprehending the complex relationship between these parameters and how they affect the characteristics of materials is essential for the progress and practical use of ceramics based on $BaTiO_3$ and other ferroelectric materials. Continuing with further research that specifically investigates the impact of grain size and its underlying processes would be advantageous for enhancing the efficiency of $BaTiO_3$-based ceramics in different applications. By improving our comprehension of these essential elements, we may create a path for developing more effective and dependable ferroelectric materials specifically designed to fulfill the requirements of developing technologies.

Acknowledgments

The author thanks the researchers supporting the project (RSPD2024R759), King Saud University, Riyadh, Saudi Arabia, for their financial support.

References

[1] Kwaaitaal, M. et al. Nature Photonics 1-5 (2024):.

[2] Xu, Yijie, Ning Liu, Ying Lin, Xingqian Mao, Hongtao Zhong, Ziqiao Chang, Mikhail N. Shneider, and Yiguang Ju. Nat. Commun 15, 3092 (2024); https://doi.org/10.1038/s41467-024-47230-7

[3] Xi, Kaibiao, Yudong Hou, Mupeng Zheng, and Mankang Zhu. Adv. Funct. Mater. 2401487 (2024).

[4] Gigli, L., Veit, M., Kotiuga, M. et al. npj Comput Mater 8, 209 (2022); https://doi.org/10.1038/s41524-022-00845-0

[5] Abbas, Waseem, Mesfin Seid Ibrahim, Muhammed Waseem, Chang Lu, Hiu Hung Lee, Shazia Fazal, K. H. Loo, and Abhijit Pramanick. J. Chem. Eng. 148943 (2024); https://doi.org/10.1016/j.cej.2024.148943

[6] A. Pramanick, A.D. Prewitt, J.S. Forrester, J.L. Jones Crit. Rev. Solid State Mater. Sci., 37 (4), 243-275 (2012); https://doi.org/10.1080/10408436.2012.686891

[7] Zhang, Ruoyun, Yueshun Zhao, Bo Yang, Shifeng Zhao. J. Phys. Chem. C, 128, 4395-4403 (2024); https://doi.org/10.1021/acs.jpcc.3c07742

[8] Deng, Caozhuang, Yi Zhang, Dan Yang, Haizhong Zhang, Minmin Zhu. Advanced Sensor Research 2300168 (2024).

[9] Radhakrishnan, J., S. Subramani, José L. Ocaña. Coordination Chemistry Reviews 502, 215621 (2024); https://doi.org/10.1016/j.ccr.2023.215621

[10] Pătru, R. E., C. A. Stanciu, E. M. Soare, R. D. Truşcă, B. S. Vasile, A. I. Nicoară, L. Trupină et al. PROG SOLID STATE CH 100457 (2024); https://doi.org/10.1016/j.progsolidstchem.2024.100457

11. Lu, Ye, Shunshun Jiang, Xinyi Zhao, Shun Guo, Ji Zhang, Kedong Zhou, Lei He, Ceram Int. 49, 37881-37887 (2023); https://doi.org/10.1016/j.ceramint.2023.09.116

12. Liu, Qing, Er Pan, Hao Deng, Fucai Liu, Jing-Feng Li, Inorganic Chemistry Frontiers 10, 2359-2369 (2023); https://doi.org/10.1039/D3QI00205E

[13] Jin, Jiao, Jiansheng Zhang, Min Shi, Chongyou Feng, Yichen Huang. J Electroceram 50, 37-43 (2023); https://doi.org/10.1007/s10832-023-00302-4

[14] Alkathy, M.S., James Raju, K.C. J Electroceram 38, 63-73 (2017); https://doi.org/10.1007/s10832-016-0060-z

[15] Bajpai, P. K., C. R. K. Mohan, K. N. Singh, Anamika Dwivedi, Milan Hait, Zhanhu Guo. ES Materials & Manufacturing 21, 861 (2023).

[16] Singh, Surinder, Anumeet Kaur, Parwinder Kaur, Lakhwant Singh. J. Alloys Compd. 941, 169023 (2023); https://doi.org/10.1016/j.jallcom.2023.169023

[17] Huang, Yunyao, Leiyang Zhang, Ruiyi Jing, Wenjing Shi, Denis Alikin, Vladimir Shur, Xiaoyong Wei, Li Jin. J. Am. Ceram. Soc. 106, 4709-4722 (2023); https://doi.org/10.1111/jace.19104

[18] Babeer, Afaf M., Abd El-razek Mahmoud, Materials Today Commu 36, 106606 (2023); https://doi.org/10.1016/j.mtcomm.2023.106606

[19] Khare, P., Sa, D. Solid State Communications, 152(16), 1572-1576 (2012); https://doi.org/10.1016/j.ssc.2012.05.019

[20] Mallick, Jyotirekha, Ajay Kumar, Tupan Das, Lagen Kumar Pradhan, Prakash Parida, Manoranjan Kar. Journal of Physics: Condensed Matter 35, 475403 (2023); https://doi.org/10.1088/1361-648X/acef9c

[21] Gupta, Sanju. J. Am. Ceram. Soc. 106, 2209-2224 (2023); https://doi.org/10.1111/jace.18874

[22] Løndal, Nora Statle, Benjamin Albert Dobson Williamson, Julian Walker, Mari-Ann Einarsrud, Tor Grande. Phys Chem Chem Phys 26, 3350-3366 (2024); https://doi.org/10.1039/D3CP05666J

[23] Kumar, Venkatramanan, Arunkumar Kathiravan, Mariadoss Asha Jhonsi. Nano Energy 109523 (2024); https://doi.org/10.1016/j.nanoen.2024.109523

[24] Li, Yang, Ting Zheng, Bing Li, Jiagang Wu. J. Am. Ceram. Soc. 106, 2393-2406 (2023); https://doi.org/10.1111/jace.18935

[25] Li, Yujing, Rongrong Rao, Yiyi Wang, Huiling Du, Jing Shi, Xiao Liu. ecs j. solid state sci. Technol. 013005 (2023); https://doi.org/10.1149/2162-8777/acb28e

[26] Li, Yang, Wei Lin, Bo Yang, Shumin Zhang, Shifeng Zhao. Acta Materialia 255, 119071 (2023); https://doi.org/10.1016/j.actamat.2023.119071

[27] Mandal, Soumen, Karsten Arts, David J. Morgan, Zhuohui Chen, Oliver A. Williams. Carbon 212, 118160 (2023); https://doi.org/10.1016/j.carbon.2023.118160

[28] Sahoo, S., T. Badapanda, D. Kumar, S. K. Rout, J. Ray, S. N. Tripathy. Journal of Molecular Structure 1308, 138006 (2024); https://doi.org/10.1016/j.molstruc.2024.138006

[29] Bhat, Showket Ahmad, Mohd Ikram, New Journal of Chemistry 48, 951-970 (2024); https://doi.org/10.1039/D3NJ05096C

[30] Mohanty, Hari Sankar, Tapendu Sundar Puhan, Sagar Padhi, Subhashree Panda, Soumya Sucharita Samantaray, Gangadhar Rana, Krishnamayee Bhoi et al. ECS J SOLID STATE SC 12, 093001 (2023); https://doi.org/10.1149/2162-8777/acf2c7

[31] Bai, Shigang, Nataliya Perevoshchikova, Yu Sha, Xinhua Wu. Applied Sciences 9, 583 (2019); https://doi.org/10.3390/app9030583

[32] C.I. Adelina, A.V. Catalina, C.M.R. Maria, et al. Mater. Char., 106, 195-207 (2015).

[33] A. Ianculescu, Z.V. Mocanu, L.P. Curecheriu, et al. J. Alloys Compd., 509, 0040-10049 (2011); https://doi.org/10.1016/j.jallcom.2011.08.027

34. Igathinathane, C., L. O. Pordesimo, et al. Computers and electronics in agriculture 63, 168-182 (2008); https://doi.org/10.1016/j.compag.2008.02.007

[35] Zhu, Rongfeng, Wanwan Ji, Bijun Fang, et al. Ceram Int 43, 6417-6424 (2017); https://doi.org/10.1016/j.ceramint.2017.02.054

[36] Chung, T. C., A. Petchsuk. Macromolecules 35, 7678-7684 (2002); https://doi.org/10.1021/ma020504c

[37] Badapanda, T., Senthil, V., Panigrahi, S. et al. J Electroceram 31, 55-60 (2013); https://doi.org/10.1007/s10832-013-9808-x

[38] B.E. Vugmeister, M.D. Glinchuk, Rev. Mod. Phys. 62, 993 (1990); https://doi.org/10.1103/RevModPhys.62.993

[39] M.T. Buscaglia, V. Buscaglia, M. Viviani, P. Nanni, M. Hanuskova, J. Eur. Ceram. Soc. 20, 1997 (2000); https://doi.org/10.1016/S0955-2219(00)00076-5

[40] K. Watanabe, H. Ohsato, H. Kishi, Y. Okino, N. Kohzu, Y. Iguchi, T. Okuda, Solid State Ion 108, 129 (1998).

[41] Chen, S., Liu, R., Zheng, Y., Shi, Y., Dang, S., Shi, Y. et al. J. Alloys Compd. 936, 168015 (2023).

[42] K. Uchino, S. Nomura, Integr. Ferroelectr. 44, 55 (1982); https://doi.org/10.1080/00150198208260644

[43] S.M. Bobade, D.D. Gulwade, A.R. Kulkarni, P. Gopalan, J. Appl. Phys. 97, 074105 (2005); https://doi.org/10.1063/1.1879074

[44] S.M. Pilgrim, A.E. Sutherland, S.R. Winzer, J. Am. Ceram. Soc. 73(10), 3122-3135 (1990); https://doi.org/10.1111/j.1151-2916.1990.tb06733.x

[45] Kimura, S. Miyamoto, T. Yamaguchi, J. Am. Ceram. Soc. 73(1), 127-130 (1990); https://doi.org/10.1111/j.1151-2916.1990.tb05102.x

[46] T. Kimura, S. Saiubol, K. Nagata, J. Ceram. Soc. Japan, Int. Ed. 103(2), 132-137 (1995); https://doi.org/10.2109/jcersj.103.132

[47] Thoret, J. Raves, Rev. Chim. Mineral. 24(3), 288-294 (1987).

[48] R. Guo, A.S. Bhalla, G. Burns, F.H. Dacol, Ferroelectrics 93, 397-405 (1989); https://doi.org/10.1080/00150198908017376

[49] Hougham, G., G. Tesoro, A., Viehbeck, J. D. Chapple-Sokol. Macromolecules 27, 5964-5971 (1994); https://doi.org/10.1021/ma00099a006

[50] Buscaglia, Maria Teresa, Massimo Viviani, et al., Phy Rev B 73, 064114 (2006).

[51] Fang, Tsang-Tse, Huey-Lin Hsieh, Fuh-Shan Shiau. J. Am. Ceram. Soc.76, 1205-1211 (1993); https://doi.org/10.1111/j.1151-2916.1993.tb03742.x

[52] Kim, Dong Hyun, Seung Jun Lee, Jayaraman Theerthagiri, Moonhee Choi, Jongsuk Jung, Yiseul Yu, Kwang Seop Im et al. Chemosphere 283, 131218 (2021); https://doi.org/10.1016/j.chemosphere.2021.131218

[53] Singh, Surinder, Anumeet Kaur et al. ACS omega 8, 5623-25638 (2023); https://doi.org/10.1021/acsomega.3c02586

[54] Lu, Da-Yong, Masayuki Toda, Mikio Sugano. J. Am. Ceram. Soc. 89(10), 3112-3123 (2006); https://doi.org/10.1111/j.1551-2916.2006.00893.x

[55] Lu, D., Gao, X., & Wang, S. Results in Physics, 12, 585-591 (2019); https://doi.org/10.1016/j.rinp.2018.11.094

[56] Butee, Sandeep, K. R. Kambale, Ajinkya Ghorpade, Abhay Halikar, Rahul Gaikwad, Himanshu Panda. J. Am. Ceram. Soc. 7(4), 407-416 (2019); https://doi.org/10.1080/21870764.2019.1656359

[57] Kuwabara, Makoto, Hirofumi Matsuda, Natsuko Kurata, Eiji Matsuyama. J. Am. Ceram. Soc. 80, 2590-2596 (1997); https://doi.org/10.1111/j.1151-2916.1997.tb03161.x

[58] Raddaoui, Z., S. El Kossi, J. Dhahri, N. Abdelmoula, K. Taibi. RSC advances 9(5), 2412-2425 (2019); https://doi.org/10.1039/C8RA08910H

[59] Ghosh, S.K., Ganguly, M., Rout, S.K. et al. Eur. Phys. J. Plus 130, 68 (2015); https://doi.org/10.1140/epjp/i2015-15154-9

[60] Gulwade, D., Gopalan, P. Solid State Commun., 146(7-8), 340-344 (2008); https://doi.org/10.1016/j.ssc.2008.02.018

[61] Yang, F., Li, Q., Zhang, A., Jia, Y., Wang, W., Fan, H. Ceram Int, 49(4), 6068-6076 (2023).

[62] Zhang, L., Wang, Z., Li, Y., Chen, P., Cai, J., Yan, Y., Zhou, Y., Wang, D., Liu, G. Eur. Ceram. Soc. 39(10), 3057-3063 (2019); https://doi.org/10.1016/j.jeurceramsoc.2019.02.004

[63] Younas, U., M. Atif, A. Anjum, M. Nadeem, T. Ali, R. Shaheen, W. Khalid, Z. Ali. RSC advances 13, 5293-5306 (2023); https://doi.org/10.1039/D2RA06640H

[64] Vijatović Petrović, M., Jelena Bobić, R. Grigalaitis, B. Stojanović, J. Banys. Acta Physica Polonica A 124, 155-160 (2013); https://doi.org/10.12693/APhysPolA.124.155

[65] R. Naik, J.J. Nazarko, C.S. Flattery, U.D. Venkateswaran, V.M. Naik, M.S. Mohammed, G.W. Auner, J.V. Mantese, N.W. Schubring, A.L. Micheli, A.B. Catalan Phys. Rev. B, 61, 11367 (2000); https://doi.org/10.1103/PhysRevB.61.11367

[66] Gulwade, D., Gopalan, P. Solid State Commun, 146(7-8), 340-344 (2008); https://doi.org/10.1016/j.ssc.2008.02.018

[67] Liu, Q., Liu, J., Lu, D., Li, T., Zheng, W. Materials, 12(4), 678 (2019); https://doi.org/10.3390/ma12040678

[68] Gong, Gaoshang, Yujiao Fang, Gebru Zerihun, Chongyang Yin, Shuai Huang, Songliu Yuan. J. Appl. Phys. 115 (2014); https://doi.org/10.1063/1.4884221